J|A|C|S ARTICLES

Published on Web 03/22/2010

Solid-State ^{17}O NMR and Computational Studies of *C*-Nitrosoarene Compounds

Gang Wu,*[,†] Jianfeng Zhu,[†] Xin Mo,[†] Ruiyao Wang,[†] and Victor Terskikh[‡]

Department of Chemistry, Queen's University, 90 Bader Lane, Kingston, Ontario, Canada K7L 3N6, and Steacie Institute for Molecular Sciences, National Research Council Canada, Ottawa, Ontario, Canada K1A 0R6

Received November 17, 2009; E-mail: gang.wu@chem.queensu.ca

Abstract: We report the first solid-state ^{17}O NMR determination of the ^{17}O quadrupole coupling (QC) tensor and chemical shift (CS) tensor for four ^{17}O-labeled *C*-nitrosoarene compounds: *p*-[^{17}O]nitroso-*N*,*N*-dimethylaniline ([^{17}O]NODMA), $SnCl_2(CH_3)_2$([^{17}O]NODMA)$_2$, $ZnCl_2$([^{17}O]NODMA)$_2$, and [^{17}O]NODMA·HCl. The ^{17}O quadrupole coupling constants (C_Q) observed in these *C*-nitrosoarene compounds are on the order of 10−15 MHz, among the largest values found to date for organic compounds. The ^{17}O CS tensor in these compounds exhibits remarkable sensitivity toward the nitroso bonding scheme with the chemical shift anisotropy ($\delta_{11} - \delta_{33}$) ranging from just 350 ppm in [^{17}O]NODMA·HCl to over 2800 ppm in [^{17}O]NODMA. This latter value is among the largest ^{17}O chemical shift anisotropies reported in the literature. These extremely anisotropic ^{17}O NMR interactions make *C*-nitrosoarene compounds excellent test cases that allow us to assess the detection limit of solid-state ^{17}O NMR. Our results suggest that, at 21.14 T, solid-state ^{17}O NMR should be applicable to all oxygen-containing organic functional groups. We also show that density functional theory (DFT) calculations can reproduce reasonably well the experimental ^{17}O QC and CS tensors for these challenging molecules. By combining quantum chemical calculations with experimental solid-state ^{17}O NMR results, we are able to determine the ^{17}O QC and CS tensor orientations in the molecular frame of reference for *C*-nitrosoarenes. We present a detailed analysis illustrating how magnetic field-induced mixing between individual molecular orbitals (MOs) contributes to the ^{17}O shielding tensor in *C*-nitrosoarene compounds. We also perform a Townes−Dailey analysis for the observed ^{17}O QC tensors and show that ^{17}O CS and QC tensors are intrinsically related through the π bond order of the N═O bond. Furthermore, we are able for the first time to examine the parallelism between individual ^{17}O and ^{15}N CS tensor components in *C*-nitrosoarenes.

1. Introduction

Oxygen is one of the most common elements found in organic and biological molecules. Oxygen-containing functional groups can be found in all biologically important molecules such as proteins, nucleic acids, carbohydrates, and phospholipids. Oxygen is often present at the center of action in many biological structures and processes. For example, oxygen-containing functional groups are directly involved around the catalytic center of many enzymes, at the ion binding sites of metalloenzymes, and at the substrate−enzyme interaction interfaces. Although the potential of ^{17}O NMR spectroscopy was recognized many years ago,[1,2] the progress has been rather slow until recently. In the past several years, significant effort has been devoted to the experimental characterization of fundamental ^{17}O quadrupole coupling (QC) and chemical shift (CS) tensors for oxygen-containing organic functional groups.[3,4]

C-nitrosoarenes represent an important class of organic compounds widely used in organic chemistry, coordination chemistry, and biochemistry.[5−7] The *C*-nitroso compounds have also found a wide range of pharmaceutical applications.[8−10] In the context of biological systems, *C*-nitrosoarenes (as well as HNO) can form stable complexes with heme proteins such as cytochrome P450, myoglobin and hemoglobin. Therefore, *C*-nitrosoarene metal complexes are also of considerable interest. Three basic binding modes are known for mononuclear *C*-nitrosoarene metal complexes;[6] see Figure 1. Although the κ^1-*N*-binding mode is the most common one, examples of κ^1-*O*-

† Queen's University.
‡ Steacie Institute for Molecular Sciences.

(1) Klemperer, W. G. *Angew. Chem., Int. Ed.* **1978**, *17*, 246–254.
(2) Kintzinger, J. P., Oxygen N. M. R. Characteristic Parameters and Applications. In *NMR Basic Principles and Progress*; Diehl, P., Fluck, E., Kosfeld, R., Eds.; Springer-Verlag: Berlin, 1981; Vol. 17, pp 1−64.
(3) Lemaitre, V.; Smith, M. E.; Watts, A. *Solid State Nucl. Magn. Reson.* **2004**, *26*, 215–235.
(4) Wu, G. *Prog. Nucl. Magn. Reson. Spectrosc.* **2008**, *52*, 118–169.
(5) Gowenlock, B. G.; Richter-Addo, G. B. *Chem. Rev.* **2004**, *104*, 3315–3340.
(6) Lee, J.; Chen, L.; West, A. H.; Richter-Addo, G. B. *Chem. Rev.* **2002**, *102*, 1019–1065.
(7) Cameron, M.; Gowenlock, B. G.; Vasapollo, G. *Chem. Soc. Rev.* **1990**, *19*, 355–79.
(8) Rice, W. G.; Schaeffer, C. A.; Harten, B.; Villinger, F.; South, T. L.; Summers, M. F.; Henderson, L. E.; Bess, J. W.; Arthur, L. O.; McDougal, J. S.; Orloff, S. L.; Mendeleyev, J.; Kun, E. *Nature* **1993**, *361*, 473–475.
(9) King, S. B., C-Nitroso compounds, oximes, N-hydroxyguanidines and N-hydroxyureas. In *Nitric Oxide Donors*; Wang, P. G., Cai, T. B., Taniguchi, N., Eds.; Wiley-VCH: Weinheim, Germany, 2005; pp 177−199.
(10) Gooden, D. M.; Chakrapani, H.; Toone, E. J. *Curr. Top. Med. Chem.* **2005**, *5*, 687–705.

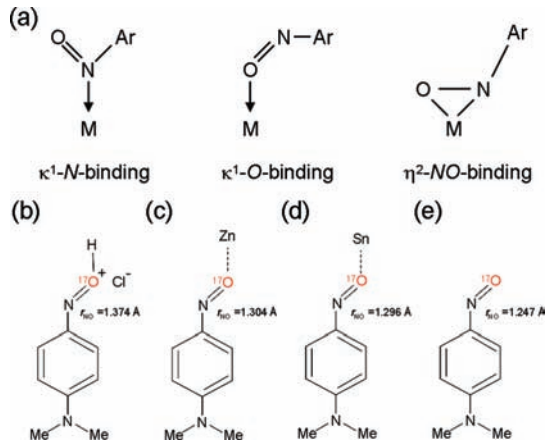

Figure 1. (a) Basic binding modes of monometallic *C*-nitrosoarene complexes. Molecular structures of the *C*-nitrosoarene compounds investigated in this study: (b) NODMA·HCl; (c) $ZnCl_2(NODMA)_2$; (d) $SnCl_2Me_2(NODMA)_2$; and (e) NODMA.

binding and η^2-*NO*-binding do exist in the literature. In particular, κ^1-*O*-binding mode has been seen in several complexes containing Zn(II), Sn(IV), Fe(III), and Mn(III) metal centers. For example, Richter-Addo and co-workers[11] reported a binding mode switch from κ^1-*N* in a ferrous [(TPP)Fe(II)(ArNO)$_2$] (TPP = *meso*-tetraphenylporphyrinato) complex to κ^1-*O* in a ferric $[(TPP)Fe(III)(ArNO)_2]^+$ complex. It appears that the κ^1-*O*-binding mode is always associated with *p*-aminosubstituted *C*-nirosoarenes in which a dipolar quinonoid resonance structure has a considerable contribution. The bidentate η^2-*NO*-binding mode has been observed in complexes containing Mo(VI), W(VI), Ru(II), Pt(II), and Cu(I) metal centers.[6,12] In addition, many polynuclear complexes such as [M$_2$](ArNO) and [M$_4$](ArNO) have also been reported in the literature.

To explore the possibility of using solid-state ^{17}O NMR as a new spectroscopic probe of the chemical bonding in *C*-nitrosoarenes and their metal complexes, we decided to determine the relevant ^{17}O NMR tensors for the ArN═O functional group, the first time such a study is undertaken. We chose to investigate four representative *C*-nitrosoarenes consisting of a parent *C*-nitrosoarene compound, its hydrochloride salt (where the N═O group is protonated) and two diamagnetic κ^1-*O*-bound metal complexes; also see Figure 1. There are three major reasons for selecting these *C*-nitrosoarene systems, especially the two κ^1-*O*-bound metal complexes, for this initial investigation. First, these compounds are diamagnetic and thus suitable for NMR studies. Second, the κ^1-*O*-binding mode should cause the largest changes in ^{17}O NMR properties as compared with those for the parent compound. Third, similar *C*-nitrosoarene compounds, in both κ^1-*N*- and κ^1-*O*-bound forms, have been investigated previously by Oldfield and co-workers[13] using solid-state ^{15}N NMR spectroscopy. Thus, a detailed comparison between ^{17}O (QC and CS) and ^{15}N (CS) NMR tensors should offer an excellent opportunity to obtain complementary information about the chemical bonding at the N═O functional group.

In the context of ^{17}O NMR spectroscopy, *C*-nitrosoarenes are known to exhibit extreme ^{17}O chemical shifts, ca. $\delta(^{17}O) \approx 1250-1550$ ppm,[14,15] primarily due to the presence of significant paramagnetic shielding contributions arising from magnetic field-induced mixing between low-lying excited states and the ground state. As a result, the ^{17}O chemical shift anisotropy is also expected to be very large in *C*-nitrosoarene compounds. In fact, the ^{15}N chemical shift anisotropies observed in *C*-nitrosoarene compounds are among the largest ever reported in the literature.[13,16,17] Although there is no literature report on the ^{17}O quadrupole coupling constant (C_Q) for *C*-nitrosoarenes, there are good reasons to believe that $C_Q(^{17}O)$ must be rather large for a nitroso group (R−N═O). For example, an aldehyde functional group (H−C═O), being isoelectronic with a nitroso group, typically has $C_Q(^{17}O)$ values of about 10−12 MHz.[18,19] Potentially, *C*-nitrosoarene compounds may pose a tremendous challenge for solid-state ^{17}O NMR studies, because a combination of very large ^{17}O quadrupole coupling constants and very large ^{17}O chemical shift anisotropies could make it exceedingly difficult to obtain high-quality ^{17}O NMR data. Not surprisingly, solid-state ^{17}O NMR studies of *C*-nitrosoarenes have never been reported in the literature. For precisely the same reasons, we believe that *C*-nitrosoarenes can be used as a test case for investigating the detection limit of solid-state ^{17}O NMR spectroscopy. We are interested in exploring the detection limit of solid-state ^{17}O NMR in two aspects. One is the sensitivity limit with respect to the largest molecular systems (e.g., proteins) for which solid-state ^{17}O NMR signals can be detected. The other is concerned with the greatest anisotropic ^{17}O NMR interactions (e.g., QC and CS tensors) for which high-quality solid-state ^{17}O NMR signals can be recorded in practice with the currently available ultrahigh magnetic fields. Recent studies by Cross and co-workers[20] and by Smith and co-workers[21] have to some extent touched upon the sensitivity issue. The present study attempts to address the second aspect. To date, the largest $C_Q(^{17}O)$ values attainable by solid-state ^{17}O NMR experiments are on the order of 11 MHz, such as those found in nitrophenols,[22] carbohydrates,[23] *p*-nitrobenzaldehyde,[24] and sodium pyruvate.[25] These $C_Q(^{17}O)$ values are still much less than the theoretical upper limit, 20.9 MHz, which is the nuclear quadrupole coupling constant expected for a single electron in the pure 2p atomic orbital of an oxygen atom.[19] As for the ^{17}O chemical shift anisotropy in organic molecules, the most anisotropic ^{17}O CS tensors so far measured have anisotropy ($\delta_{11} - \delta_{33}$) on the order of 1000−3000 ppm, such as those found in

(11) Wang, L.-S.; Chen, L.; Khan, M. A.; Richter-Addo, G. B. *Chem. Commun.* **1996**, 323–324.
(12) Wiese, S.; Kapoor, P.; Williams, K. D.; Warren, T. H. *J. Am. Chem. Soc.* **2009**, *131*, 18105–18111.
(13) Salzmann, R.; Wojdelski, M.; McMahon, M.; Havlin, R. H.; Oldfield, E. *J. Am. Chem. Soc.* **1998**, *120*, 1349–1356.
(14) Orrell, K. G.; Sik, V.; Stephenson, D. *Magn. Reson. Chem.* **1987**, *25*, 1007–1011.
(15) Dahn, H.; Pechy, P.; Flogel, R. *Helv. Chim. Acta* **1994**, *77*, 306–316.
(16) Lumsden, M. D.; Wu, G.; Wasylishen, R. E.; Curtis, R. D. *J. Am. Chem. Soc.* **1993**, *115*, 2825–2832.
(17) Mason, J.; Larkworthy, L. F.; Moore, E. A. *Chem. Rev.* **2002**, *102*, 913–934.
(18) Flygare, W. H.; Lowe, J. T. *J. Chem. Phys.* **1965**, *43*, 3645–3653.
(19) Cheng, C. P.; Brown, T. L. *J. Am. Chem. Soc.* **1979**, *101*, 2327–2334.
(20) Hu, J.; Chekmenev, E. Y.; Gan, Z.; Gor'kov, P. L.; Saha, S.; Brey, W. W.; Cross, T. A. *J. Am. Chem. Soc.* **2005**, *127*, 11922–11923.
(21) Wong, A.; Beevers, A. J.; Kukol, A.; Dupree, R.; Smith, M. E. *Solid State Nucl. Magn. Reson.* **2008**, *33*, 72–75.
(22) Dong, S.; Yamada, K.; Wu, G. *Z. Naturforsch. A* **2000**, *55*, 21–28.
(23) Sefzik, T. H.; Houseknecht, J. B.; Clark, T. M.; Prasad, S.; Lowary, T. L.; Gan, Z.; Grandinetti, P. J. *Chem. Phys. Lett.* **2007**, *434*, 312–315.
(24) Wu, G.; Mason, P.; Mo, X.; Terskikh, V. *J. Phys. Chem. A* **2008**, *112*, 1024–1032.
(25) Zhu, J.; Geris, A. J.; Wu, G. *Phys. Chem. Chem. Phys.* **2009**, *11*, 6972–6980.

[$^{17}O_2$]picket fence porphyrin,[26] metal nitrosyls,[27] *p*-nitrobenzaldehyde,[24] and sodium pyruvate.[25] Among these cases, however, there have been only two instances so far, *p*-nitrobenzaldehyde and sodium pyruvate, where very large ^{17}O quadrupole coupling constant and chemical shift anisotropy are present *simultaneously*. As we argued earlier, *C*-nitrosoarenes may represent an even more challenging case.

2. Experimental Section

Synthesis. All common chemicals and solvents were purchased from Sigma-Aldrich (Oakville, Ontario, Canada). Water (70% ^{17}O atom) was purchased from isoSolutions (Ottawa, Ontario, Canada). *p*-[^{17}O]nitroso-*N*,*N*-dimethylaniline ([^{17}O]NODMA)was prepared by the following procedure. Approximately 300 mg of *N*,*N*-dimethylaniline was dissolved in 1 mL of concentrated hydrochloric acid (33% HCl in ^{17}O-enriched water) followed by slow addition of a solution of 180 mg of sodium nitrite in 0.3 mL of ^{17}O-enriched water, while maintaining the solution at 5 °C and stirring. After keeping the orange mixture at 5 °C for 1 h, solid NaOH was added until the solution became bright green. The excessive ^{17}O-enriched water was then recovered on a vacuum line. The solid residue was washed with 3 × 1 mL water. Recrystallization from 3 mL of 50% ethanol aqueous solution yielded 219 mg of *p*-[^{17}O]nitroso-*N*,*N*-dimethylaniline (yield, 59%) as a dark-green polycrystalline solid. *p*-[^{17}O]nitroso-*N*,*N*-dimethylaniline hydrochloride monohydrate was obtained by recrystallization of [^{17}O]NODMA from 2 M HCl(aq). $ZnCl_2$(*p*-[^{17}O]nitroso-*N*,*N*-dimethylaniline)$_2$ and $SnCl_2(CH_3)_2$(*p*-[^{17}O]nitroso-*N*,*N*-dimethylaniline)$_2$ were prepared from [^{17}O]NODMA by the literature methods.[28,29] Solution ^1H and ^{13}C NMR spectra of these compounds were obtained to confirm the purity of the synthesized products. The ^{17}O enrichment level in the final products was estimated to be approximately 55% using solution ^{17}O NMR.

Solid-State ^{17}O NMR. Solid-state ^{17}O NMR spectra were recorded at 11.74 and 21.14 T, operating at the ^{17}O Larmor frequencies of 67.78 and 122.02 MHz, respectively. At 11.74 T, a 4 mm MAS probe was used to obtain ^{17}O NMR spectra for stationary powder samples. At 21.14 T, a 3.2 mm MAS probe was used in acquiring static spectra. For MAS experiments, a 2.5 mm MAS probe was used with a sample spinning frequency of 35 kHz. High power ^1H decoupling was used in all cases. Other experimental details are given in figure captions. Spectral simulations were performed using WSOLIDS[30] and DMFit[31] simulation programs.

X-ray Crystallography. A red, block-shaped single crystal of $SnCl_2(CH_3)_2$(*p*-nitroso-*N*,*N*-dimethylaniline)$_2$ (0.281 × 0.168 × 0.166 mm^3) was mounted on a glass fiber with grease and cooled to −93 °C in a stream of nitrogen gas controlled with Cryostream Controller 700. Data collection was performed on a Bruker SMART APEX II X-ray diffractometer with graphite-monochromated Mo K_α radiation ($\lambda = 0.71073$ Å), operating at 50 kV and 30 mA over 2θ ranges of 4.58−50.00°. No significant decay was observed during the data collection. Data were processed on a PC using the Bruker AXS Crystal Structure Analysis Package.[32] Neutral atom scattering factors were taken from Cromer and Waber.[33] The crystal is triclinic space group $P\bar{1}$, based on the systematic absences, *E* statistics, and successful refinement of the structure. The structure was solved by direct methods. Full-matrix least-squares refinements minimizing the function $\sum w (F_o^2 - F_c^2)^2$ were applied to the compound. All non-hydrogen atoms were refined anisotropically. The hydrogen atoms were calculated, and their contributions were included in the structure factor calculations. Convergence to final $R_1 = 0.0151$ and $wR_2 = 0.0374$ for 1822 ($I > 2\sigma(I)$) independent reflections, and $R_1 = 0.0153$ and $wR_2 = 0.0375$ for all 1839 (R(int) = 0.0135) independent reflections, with 218 parameters and 0 restraints, were achieved. The largest residual peak and hole were found to be 0.373 and −0.242 e/Å^3, respectively.

Quantum Chemical Calculations. Calculations of ^{17}O (QC and CS), ^{15}N (CS) and ^{14}N (QC) NMR tensors were performed using density functional theory (DFT) methods as implemented in Amsterdam Density Functional (ADF)[34,35] and Gaussian03 (G03)[36] programs. In the ADF calculations, Vosko−Wilk−Nusair (VWN) exchange-correlation functional[37] was used for the local density approximation (LDA) and Perdew−Burke−Ernzerhof (PBE) exchange-correlation functional[38] was applied for the generalized gradient approximation (GGA). Standard Slater-type-orbital (STO) basis sets with triple-ξ quality plus different numbers of polarization functions (TZP and TZ2P) were used for all atoms except for Sn. The QZ4P basis set was used for Sn. The relativistic (scalar) effect was included using either zeroth-order regular approximation (ZORA)[39,40] or Pauli-type[41] Hamiltonians. Mayer bond orders for the N═O group were calculated using the keyword "EXTENDEDPOPAN" and the TZ2P basis set. In the G03 calculations, the hybrid B3LYP exchange functional[42,43] was used with standard basis sets such as 6-311G(d,p), 6-311++G(d,p), 6-311++G(3df,3pd), and cc-pVTZ. In both ADF and G03 shielding calculations, the gauge-including atomic orbital (GIAO) approach[44,45] was employed. All quantum mechanical calculations were performed on Sun Fire E25K servers running Solaris 10, each with 72 dual-core UltraSPARC-IV+ 1.5 GHz SMP processors and 576 GB of RAM. Typically six processors were used for each calculation.

The principal components of the electric field gradient (EFG) tensor, eq_{ii} ($ii = xx, yy, zz$; $|eq_{zz}| > |eq_{yy}| > |eq_{xx}|$ and $eq_{zz} + eq_{yy} + eq_{xx} = 0$), were computed in atomic units (1 au = 9.717365 × 10^{21} V m^{-2}). The principal components of the shielding tensor (σ_{ii}) were reported using the usual convention: $\sigma_{iso} = (\sigma_{11} + \sigma_{22} + \sigma_{33})/3$ and $\sigma_{33} > \sigma_{22} > \sigma_{11}$. In solid-state NMR experiments for quadrupolar nuclei, the measurable quantities for a quadrupole coupling (QC)

(26) Oldfield, E.; Lee, H. C.; Coretsopoulos, C.; Adebodun, F.; Park, K. D.; Yang, S. T.; Chung, J.; Phillips, B. *J. Am. Chem. Soc.* **1991**, *113*, 8680–8685.
(27) Godbout, N.; Sanders, L. K.; Salzmann, R.; Havlin, R. H.; Wojdelski, M.; Oldfield, E. *J. Am. Chem. Soc.* **1999**, *121*, 3829–3844.
(28) Hu, S.; Thompson, D. M.; Ikekwere, P. O.; Barton, R. J.; Johnson, K. E.; Robertson, B. E. *Inorg. Chem.* **1989**, *28*, 4552–4554.
(29) Matsubayashi, G.-E.; Nakatsu, K. *Inorg. Chim. Acta* **1982**, *64*, L163–L164.
(30) Eichele, K.; Wasylishen, R. E. WSOLIDS1: Solid-State NMR Spectrum Simulation, Version 1.19.11; Universität Tübingen: Tübingen, Germany2009.
(31) Massiot, D.; Fayon, F.; Capron, M.; King, I.; Le Calve, S.; Alonso, B.; Durand, J.-O.; Bujoli, B.; Gan, Z.; Hoatson, G. *Magn. Reson. Chem.* **2002**, *40*, 70–76.
(32) *Bruker AXS Crystal Structure Analysis package: SHELXTL (Version 6.14), XPREP (Version2005/2), SAINT (Version 7.23A), APEX2 (Version 2.0−.2)*; Bruker AXS Inc.: Madison, Wisconsin, USA.
(33) Cromer, D. T.; Waber, J. T., *International Tables for X-ray Crystallography*; Kynoch Press: Birmingham, U.K., 1974.
(34) *ADF2006, SCM*; Theoretical Chemistry, Vrije University; Amsterdam, the Netherlands; http://www.scm.com.
(35) Te Velde, G.; Bickelhaupt, F. M.; Baerends, E. J.; Fonseca Guerra, C.; Van Gisbergen, S. J. A.; Snijders, J. G.; Ziegler, T. *J. Comput. Chem.* **2001**, *22*, 931–967.
(36) Frisch, M. J.; et al. *Gaussian 03*, Revision C.02; Gaussian, Inc.: Wallingford, CT, 2004.
(37) Vosko, S. H.; Wilk, L.; Nusair, M. *Can. J. Phys.* **1980**, *58*, 1200–1211.
(38) Perdew, J. P.; Burke, K.; Ernzerhof, M. *Phys. Rev. Lett.* **1996**, *77*, 3865–3868.
(39) van Lenthe, E.; Baerends, E. J.; Snijders, J. G. *J. Chem. Phys.* **1993**, *99*, 4597–4610.
(40) van Lenthe, E.; Baerends, E. J.; Snijders, J. G. *J. Chem. Phys.* **1994**, *101*, 9783–9792.
(41) Schreckenbach, G.; Ziegler, T. *Int. J. Quantum Chem.* **1997**, *61*, 899–918.
(42) Becke, A. D. *J. Chem. Phys.* **1993**, *98*, 5648–5652.
(43) Lee, C. T.; Yang, W. T.; Parr, R. G. *Phys. Rev. B* **1988**, *37*, 785–789.
(44) Ditchfield, R. *Mol. Phys.* **1974**, *27*, 789–807.
(45) Wolinski, K.; Hilton, J. F.; Pulay, P. *J. Am. Chem. Soc.* **1990**, *112*, 8251–8260.

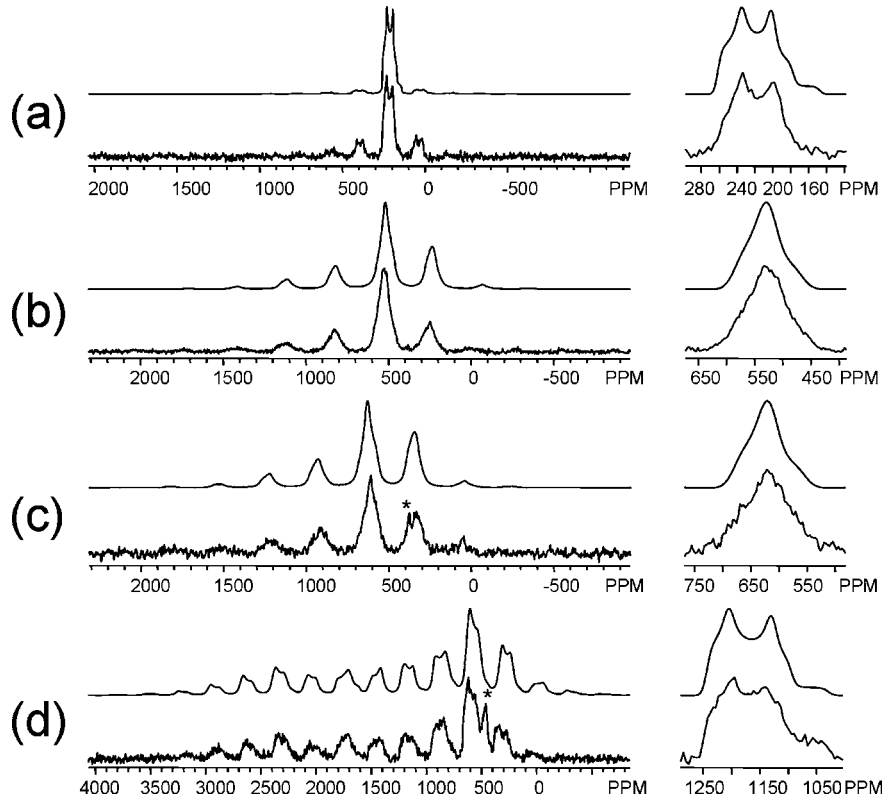

Figure 2. Experimental (lower trace) and simulated (upper trace) ^{17}O MAS spectra (left column) and "total" MAS line shapes (right column) of (a) [^{17}O]NODMA·HCl, (b) $ZnCl_2$([^{17}O]NODMA)$_2$, (c) $SnCl_2Me_2$([^{17}O]NODMA)$_2$, and (d) [^{17}O]NODMA. All spectra were recorded at 21.14 T. The sample spinning frequency was (a) 22 kHz and (b, c, d) 35 kHz. Detailed acquisition parameters were: (a) 3862 transients, 5 s recycle time; (b) 28000 transients, 2 s recycle time; (c) 36000 transients, 2 s recycle time; (d) 36148 transients, 2 s recycle time. The sharp peaks marked by * are due to ZrO_2 rotor and a trace amount of ^{17}O-labeled $NaNO_2$ in (c) and (d), respectively.

Table 1. Experimental ^{17}O QC and CS Tensors Determined for *C*-Nitrosoarene Compounds

compound	δ_{iso} (ppm)[a]	$\lvert C_Q\rvert$(MHz)[a]	η_Q[a]	δ_{11} (ppm)[b]	δ_{22} (ppm)[b]	δ_{33} (ppm)[b]	α (deg)[b]	β (deg)[b]	γ (deg)[b]
[^{17}O]NODMA·HCl	263 ± 5	10.8 ± 0.5	0.4 ± 0.1	450 ± 10	260 ± 10	100 ± 10	90 ± 10	90 ± 2	50 ± 10
$ZnCl_2$([^{17}O]NODMA)$_2$	600 ± 5	9.6 ± 0.5	1.0 ± 0.1	1260 ± 10	480 ± 10	60 ± 10	6 ± 10	88 ± 2	74 ± 10
$SnCl_2Me_2$([^{17}O]NODMA)$_2$	717 ± 5	10.5 ± 0.5	0.9 ± 0.1	1450 ± 10	600 ± 10	100 ± 10	0 ± 10	89 ± 2	74 ± 10
[^{17}O]NODMA	1200 ± 5	15.0 ± 0.5	0.3 ± 0.1	2900 ± 10	750 ± 10	100 ± 10	18 ± 10	90 ± 2	83 ± 10

[a] Obtained from analysis of MAS spectra. [b] Obtained from analysis of static spectra.

tensor (χ_{ii} where $ii = xx, yy, zz$; $|\chi_{zz}| > |\chi_{yy}| > |\chi_{xx}|$ and $\chi_{zz} + \chi_{yy} + \chi_{xx} = 0$) are nuclear quadrupole coupling constant (C_Q) and asymmetry parameter (η_Q). To compare calculated EFG tensors with experimental QC tensors, following equations were used:

$$C_Q[\mathrm{MHz}] = e^2 q_{zz} Q/h = \chi_{zz} = 243.96 \times Q[\mathrm{barn}] \times e q_{zz}[\mathrm{au}] \quad (1)$$

$$\eta_Q = (\chi_{xx} - \chi_{yy})/\chi_{zz} = (q_{xx} - q_{yy})/q_{zz} \quad (2)$$

where Q is the nuclear quadrupole moment, e is the elementary charge, and h is the Planck constant. In this study, we used $Q(^{17}\mathrm{O}) = -2.558$ and $Q(^{14}\mathrm{N}) = 2.044$ barn (1 barn $= 10^{-28}$ m^2).[46] To make direct comparison between the calculated shielding values, σ, and the observed chemical shifts, δ, we used the established shielding scales:

$$\delta(\mathrm{ppm}) = \sigma_{ref}(\mathrm{ppm}) - \sigma(\mathrm{ppm}) \quad (3)$$

where $\sigma_{ref} = 287.5$ ppm[47] and 244.6 ppm[48] for ^{17}O and ^{15}N nuclei, respectively.

3. Results and Discussion

Analysis of ^{17}O MAS spectra. Figure 2 shows the experimental and simulated ^{17}O MAS spectra for *C*-nitrosoarene compounds at 21.14 T. In most cases, strong spinning sidebands were observed even at a sample spinning frequency of 35 kHz, indicating the presence of significant ^{17}O chemical shift anisotropy. For example, the spinning sidebands observed for [^{17}O]NODMA span a range of approximately 3000 ppm (~350 kHz at 21.14 T). To analyze these "slow" MAS spectra, we first obtained the "total" MAS line shape for each compound by adding all the spinning sidebands onto the central band, as also shown in Figure 2. From each "total" MAS line shape, three ^{17}O NMR spectral parameters (δ_{iso}, $|C_Q|$, η_Q) can be obtained in a straightforward fashion. Table 1 lists the results from such an analysis for the four *C*-nitrosoarenes. It can be

(46) Pyykko, P. *Mol. Phys.* **2008**, *106*, 1965–1974.
(47) Wasylishen, R. E.; Bryce, D. L. *J. Chem. Phys.* **2002**, *117*, 10061–10066.
(48) Jameson, C. J.; Jameson, A. K.; Oppusunggu, D.; Wille, S.; Burrell, P. M.; Mason, J. *J. Chem. Phys.* **1981**, *74*, 81–88.

seen immediately that the observed δ_{iso} values are drastically different among the four *C*-nitrosoarene compounds, reflecting the nature of chemical bonding around the nitroso (N═O) group. It is quite remarkable to see that protonation of the nitroso group causes a change in the ^{17}O isotropic chemical shift of ~1000 ppm! For the two *O*-bonded *C*-nitrosoarene metal complexes, coordination of the nitroso group to a metal center has also resulted in very large ^{17}O isotropic chemical shift changes, ~500−600 ppm. The values of $C_Q(^{17}O)$ observed for the four *C*-nitrosoarenes are between 9.6 and 15 MHz. These values are among the largest so far experimentally measured by solid-state ^{17}O NMR.[4] As also seen from Figure 2, the observed spinning sidebands can be reproduced reasonably well by spectral simulations. However, as we have mentioned before,[24] we recommend to examine spinning sideband patterns only *after* the ^{17}O CS tensor components are obtained from analyses of static ^{17}O NMR spectra.

Analysis of ^{17}O Static Spectra. To obtain further information about the ^{17}O CS tensor components and their relative orientations with respect to the ^{17}O QC tensor, we performed ^{17}O NMR experiments for nonspinning (stationary) powder samples at two magnetic fields, 11.74 and 21.14 T. The static ^{17}O NMR spectra shown in Figure 3 are of excellent quality, even though in some cases the spectral widths exceed 300 kHz. Because the ^{17}O isotropic chemical shift (δ_{iso}) and quadrupole parameters ($|C_Q|$ and η_Q) have been determined in the previous section, the remaining spectral parameters to be determined are two independent CS tensor components and three Euler angles (α, β, γ) that define the relative orientation between the CS and QC tensors. In practice, we often use the tensor orientations obtained from high-level quantum chemical calculations as a starting point in spectral simulation. In most cases, we found that these initial Euler angles do not require significant changes. Under such a circumstance, one just needs to find the values for two independent CS tensor components that would *simultaneously* fit the static ^{17}O NMR spectra obtained at two magnetic fields. A more detailed description about spectral analysis for static ^{17}O NMR spectra can be found in one of our earlier publications.[49] Complete solid-state ^{17}O NMR results obtained for the four *C*-nitrosoarene compounds are summarized in Table 1. As expected, the large δ_{iso} value observed for [^{17}O]NODMA is associated with a remarkably large ^{17}O chemical shift anisotropy ($\delta_{11} - \delta_{33} = 2800$ ppm). At the other extreme, the ^{17}O CS tensor in [^{17}O]NODMA·HCl exhibits a rather small chemical shift anisotropy, $\delta_{11} - \delta_{33} = 350$ ppm. We can also see from Table 1 that δ_{11} and δ_{22} tensor components can change significantly, whereas δ_{33} values remain essentially invariant. This trend is in line with the previous observations for carbonyl compounds.[24] As mentioned earlier, after we obtained the ^{17}O CS tensor components and their relative orientations, we were able to simulate the spinning sideband patterns in the MAS spectra; see Figure 2. The simulated spinning sideband patterns match closely with the experimental spectra, providing further confirmation about the reliability of the solid-state ^{17}O NMR parameters reported in Table 1.

At this point, it is important to point out that, because $SnCl_2Me_2(NODMA)_2$ and $ZnCl_2(NODMA)_2$ have $\eta_Q \approx 1$, there exist two sets of Euler angles that can produce rather similar (but not identical) ^{17}O NMR spectra. In the present cases, the two sets of Euler angles are related by $\alpha_1 = \alpha_2 \approx 0°$, $\beta_1 = \beta_2 \approx 90°$, and $\gamma_1 = 90° - \gamma_2$. These two sets of Euler angles describe such tensor orientations that, in one case, δ_{11} is roughly along the direction of χ_{yy}, whereas in the other case, δ_{11} is roughly along the direction of χ_{zz}. The origin of this ambiguity is quite easy to understand. When a QC tensor has $\eta_Q \approx 1$, χ_{zz} and χ_{yy} components would have very similar magnitude but opposite signs. Because NMR spectra are independent of the absolute signs of the QC tensor components, these two sets of Euler angles in fact describe essentially the same physical situation, thus producing very similar static and MAS spectra. This is a general problem often encountered whenever the QC tensor under study has $\eta_Q \approx 1$. Therefore, caution should be exercised in deciding which set of the Euler angles is the correct one (*vide infra*).

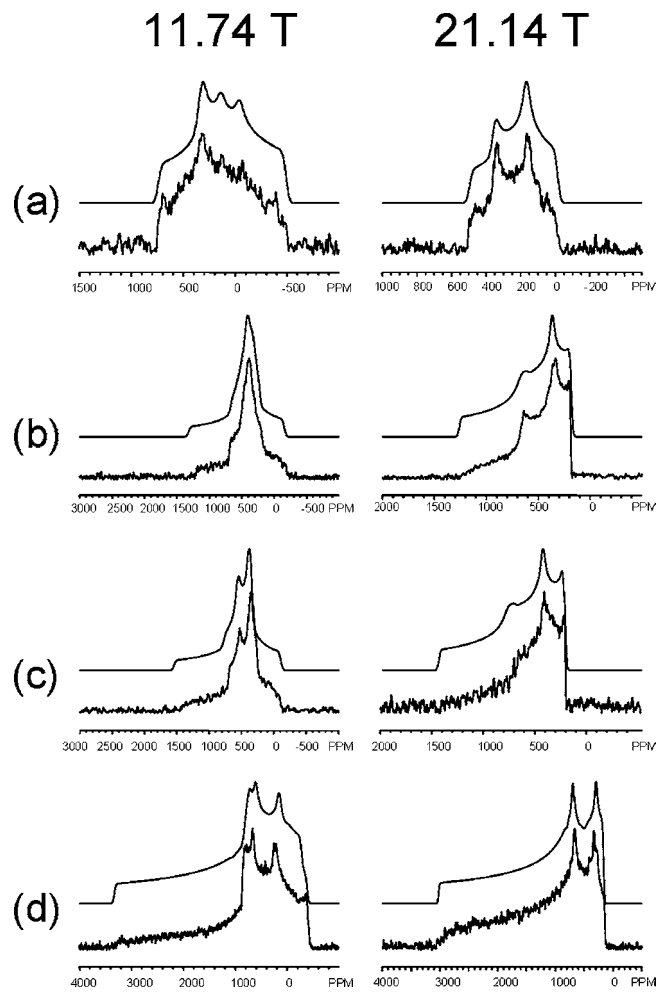

Figure 3. Experimental (lower trace) and simulated (upper trace) ^{17}O NMR spectra for stationary powder samples of (a) [^{17}O]NODMA·HCl, (b) $ZnCl_2([^{17}O]NODMA)_2$, (c) $SnCl_2Me_2([^{17}O]NODMA)_2$, and (d) [$^{17}O$]NODMA obtained at 11.74 T (left column) and 21.14 T (right column). Detailed experimental parameters are given below. For data collected at 11.74 T: (a) 6912 transients, 10 s recycle time; (b) 5198 transients, 10 s recycle time; (c) 123602 transients, 1 s recycle time; (d) 35384 transients, 2 s recycle time. For data collected at 21.14 T: (a) 6563 transients, 2 s recycle time; (b) 30578 transients, 2 s recycle time; (c) 35204 transients, 2 s recycle time; (d) 12631 transients, 2 s recycle time.

Crystal Structure of $SnCl_2Me_2(NODMA)_2$. Before we present further ^{17}O NMR results and quantum chemical computations, in this section we describe a revised crystal structure of $SnCl_2Me_2(NODMA)_2$. The crystal structure of $SnCl_2Me_2(NODMA)_2$ was first reported in 1982 by Matsubayashi and Nakatsu[29] in which the N═O bond length was found to be

(49) Yamada, K.; Dong, S.; Wu, G. *J. Am. Chem. Soc.* **2000**, *122*, 11602–11609.

Table 2. Calculated ^{17}O (CS and QC), ^{15}N (CS) and ^{14}N (QC) NMR Tensors for *C*-Nitrosoarene Compounds. Experimental Results from Solid-State ^{17}O[a] and ^{15}N[b] NMR and ^{14}N[c] NQR Measurements Are Also Listed for Easy Comparison

		^{17}O						^{15}N				^{14}N	
compound	method	δ_{iso} (ppm)	δ_{11} (ppm)	δ_{22} (ppm)	δ_{33} (ppm)	C_Q (MHz)[f]	η_Q	δ_{iso} (ppm)	δ_{11} (ppm)	δ_{22} (ppm)	δ_{33} (ppm)	C_Q (MHz)	η_Q
NODMA	ADF[d]	1552	3933	742	−18	15.7	0.06	918	2111	511	131	−6.391	0.479
	G03/B3LYP[e]	1523	3784	806	−21	16.5	0.03	943	2153	554	122	−6.934	0.563
	(exptl)	1250	2900	750	100	15.0	0.3	802	1692	537	175	−5.825	0.488
$SnCl_2Me_2(NODMA)_2$	ADF[d]	919	1927	700	130	10.9	0.68	679	1382	514	140	−6.376	0.276
	G03/B3LYP[e]	935	2002	728	74	12.2	0.63	772	1638	556	122	−7.262	0.430
	(exptl)	717	1450	600	100	10.5	0.9	596	1174	472	145	—	—
$ZnCl_2(NODMA)_2$	ADF[d]	1001	2245	709	50	12.0	0.58	772	1653	525	138	−6.605	0.308
	G03/B3LYP[e]	968	2136	735	32	13.5	0.55	813	1744	569	125	−7.205	0.444
	(exptl)	600	1260	480	60	9.6	1.0	583	1165	445	141	—	—
NODMA·HCl	ADF[d]	272	569	177	71	−11.5	0.31	502	915	417	174	−6.512	0.255
	G03/B3LYP[e]	263	558	158	74	−12.2	0.38	516	946	437	166	−6.910	0.158
	(exptl)	270	450	260	100	−10.8	0.4	429	747	394	146	—	—

[a] This work. [b] From ref 13. [c] From ref 50. [d] Computed with TZ2P basis set and a relativistic Pauli-type Hamiltonian. [e] Computed with the 6-311++G(3df,3pd) basis set for nonmetal atoms and the DZVP basis set for metal atoms. [f] The sign of experimental C_Q was assumed to be the same as the calculated ones.

1.218(4) Å. As Oldfield and co-workers[13] noted previously, this N═O bond length is unusually short and most likely results from experimental errors. For this reason, we decided to re-examine the crystal structure of this compound. New crystallographic data and structural details for $SnCl_2Me_2(NODMA)_2$ are provided in the Supporting Information. Although the unit cell parameters determined by us are quite similar to those reported by Matsubayashi and Nakatsu,[29] we did observe a significant disorder phenomenon that had not been mentioned in the previous study. As shown in Figure S1 (Supporting Information), the two symmetry-related NODMA molecules can orient themselves in two different ways related by a two-fold axis through the metal center. We found that the two orientations have an occupancy ratio of about 3:1. The N═O bond lengths are 1.296(4) and 1.283(15) Å for the major (75%) and minor (25%) orientations, respectively. These N═O bond lengths are significantly longer than 1.218 Å, but consistent with those found in other nitroso−metal complexes, e.g., 1.304 Å in $ZnCl_2(NODMA)_2$.[28] These new crystallographic results suggest that it was the unsolved disorder that had led to the erroneous N═O bond length reported by Matsubayashi and Nakatsu.[29] In a broader context, significant crystallographic disorder is commonly observed in κ^1-*O*-bonded *C*-nitroso complexes; many reported N═O bond distances in the literature may need to be re-examined.[6] In the next sections, we use this correct crystal structure to build molecular models of $SnCl_2Me_2(NODMA)_2$ for quantum chemical calculations.

Calculations of ^{17}O and $^{14/15}N$ NMR tensors. In this section, we present results of extensive DFT computations for *C*-nitrosoarenes and their metal complexes. Because ^{15}N CS and ^{14}N QC tensors have been previously reported for these *C*-nitrosoarene compounds in the literature,[13,50] we decided to examine ^{17}O (QC and CS), ^{14}N (QC) and ^{15}N (CS) NMR tensors in a unified fashion. This would allow us to fully assess the quality of quantum chemical computations. We performed two types of DFT calculations. One is to use the exchange functional built in the ADF package and the other to employ the hybrid exchange functional B3LYP as implemented in the G03 suite of programs. We have performed calculations using a variety of standard basis sets and different spin−orbit relativistic methods. For NODMA, $ZnCl_2(NODMA)_2$ and NODMA·HCl, we used the crystal structures from the literature.[28,51,52] For $SnCl_2Me_2(NODMA)_2$, we used the revised crystal structure reported in the previous section. In this case, because the two ligand orientations due to crystallographic disorder are associated with slightly different molecular structures, we performed calculations on both of them. We found that the computed results are quite similar for the major (75% occupancy) and minor (25% occupancy) components (within 1% and 8% for the QC and CS tensor components, respectively). Therefore, we report only those from the major component. Some representative results are listed in Table 2; a complete list of results for all basis sets and methods used in this study can be found in the Supporting Information. Figure 4 shows comparison between experimental and computed CS and QC tensor components for the four *C*-nitrosoarene compounds. In general, ADF and B3LYP/G03 methods reproduce the experimental NMR data to a similar degree of accuracy. For the ^{17}O and ^{14}N QC tensor components, both ADF and B3LYP/G03 methods are able to reproduce the experimental results within 10%. It is also well-known that even better agreement can be achieved if "calibrated" *Q* values are used.[53−57] It is worth mentioning that the value of $C_Q(^{14}N)$, −5.825 MHz, reported for NODMA from a nuclear quadrupole resonance (NQR) study,[50] is also among the largest values known for ^{14}N nuclei.[17,58−60] For the ^{17}O and ^{15}N CS tensors, although calculations reproduce the general trend, they nonetheless overestimate the experimental chemical shift values by approximately 40%. This is a general phenomenon that results exclusively from overestimation of the paramagnetic shielding contributions (in magnitude) in molecular systems by most computational methods. On the other hand, *C*-nitrosoarenes represent a very challenging class of molecules on their own where substantial electron correlation effects in the N═O group

(50) Beepath, N.; Stephenson, D. *Hyperfine Interact.* **2004**, *159*, 137–141.
(51) Romming, C.; Talberg, H. J. *Acta Chem. Scand.* **1973**, *27*, 2246–2248.
(52) Drangfelt, O.; Romming, C. *Acta Chem. Scand.* **1974**, *28*, 1101–1105.
(53) Eggenberger, R.; Gerber, S.; Huber, H.; Searles, D.; Welker, M. *J. Mol. Spectrosc.* **1992**, *151*, 474–481.
(54) Ludwig, R.; Weinhold, F.; Farrar, T. C. *J. Chem. Phys.* **1996**, *105*, 8223–8230.
(55) Bailey, W. C. *Chem. Phys. Lett.* **1998**, *292*, 71–74.
(56) Dong, S.; Ida, R.; Wu, G. *J. Phys. Chem. A* **2000**, *104*, 11194–11202.
(57) Wu, G.; Hook, A.; Dong, S.; Yamada, K. *J. Phys. Chem. A* **2000**, *104*, 4102–4107.
(58) Lucken, E. A. C. *Nuclear Quadrupole Coupling Constants*; Academic Press: New York, 1969.
(59) Edmonds, D. T. *Phys. Rep.* **1977**, *29C*, 233–290.
(60) Smith, J. A. S. *Chem. Soc. Rev.* **1986**, *15*, 225–260.

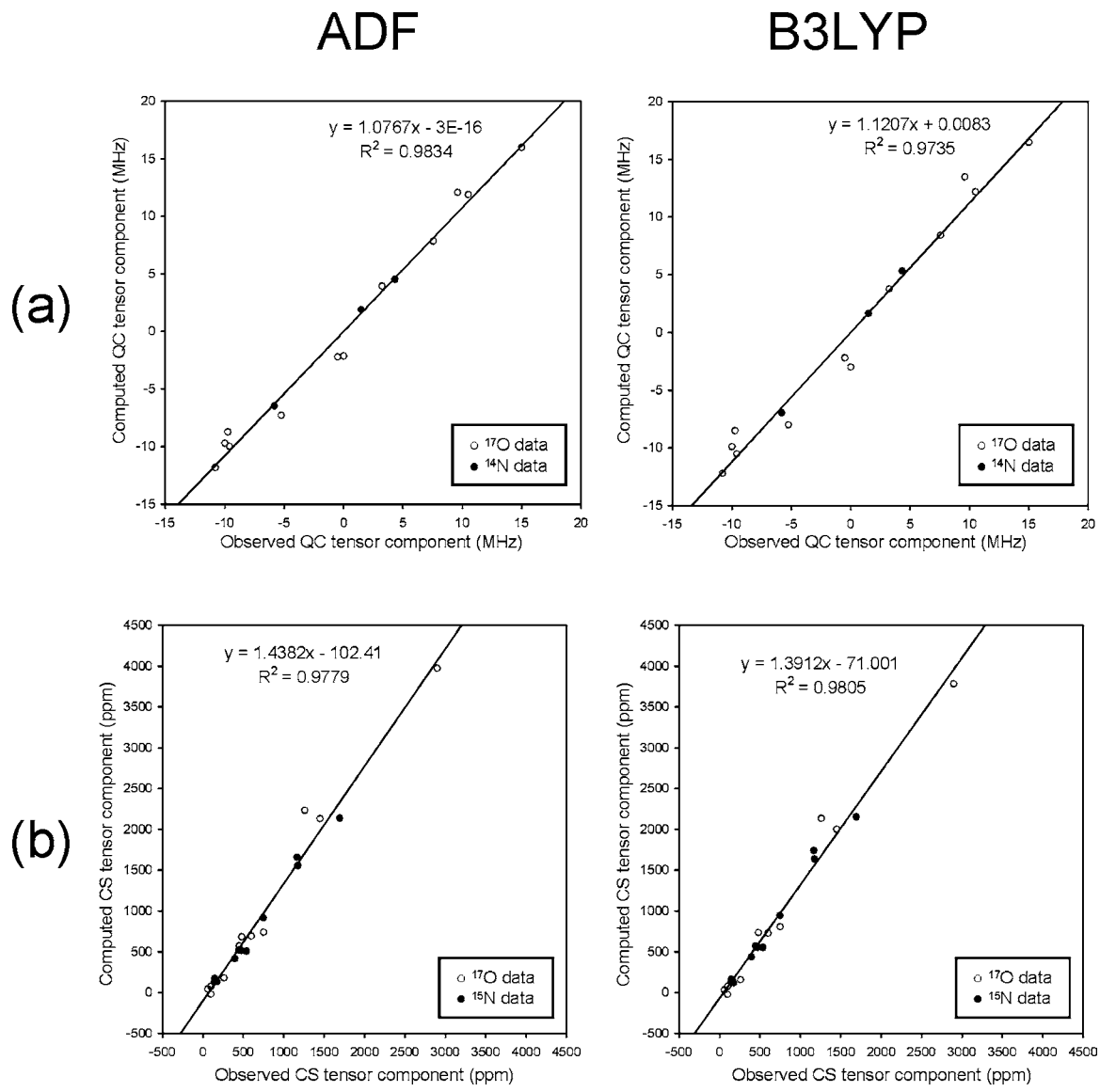

Figure 4. Comparison between experimental and calculated NMR tensor components for *C*-nitrosoarene compounds. (a) ^{17}O and ^{14}N QC tensor components and (b) ^{17}O and ^{15}N CS tensor components.

are expected. Given that the current data set covers nearly the entire chemical shift ranges for ^{17}O and ^{15}N nuclei, the computed results shown in Figure 4 are indeed very encouraging. It is particularly satisfying to see in Figure 4 that all ^{17}O, ^{14}N and ^{15}N NMR tensors behave in a similar fashion, suggesting that the current computational methods are valid. The observed systematic discrepancy in the computed CS tensor components for *C*-nitrosoarene compounds is somewhat larger than that seen in carbonyl compounds.[24,49,61−66] This is not surprising because the ^{17}O chemical shift anisotropy observed in a N═O group is more than twice of that seen in a C═O group. Fortunately, once this systematic discrepancy is identified, it is possible to make appropriate corrections so that these computational methods can yield more precise ^{17}O CS tensors in other oxygen-containing functional groups.

To further examine the dependence of ^{17}O NMR tensors on the binding mode of *C*-nitrosoarene metal complexes, we performed quantum chemical calculations on the ^{17}O NMR tensors in Fe(TPP)(Py)(NODMA)[27] and Pt(Ph_3P)$_2$(PhNO),[67] which can be considered as representative models for κ^1-*N*- and η^2-*N*-binding modes, respectively; see Figure 1. The computational results suggest that both ^{17}O QC and CS tensors are remarkably sensitive to the way that the nitroso group is bound to the metal center. In particular, the value of $\delta_{iso}(^{17}O)$ changes drastically: κ^1-*N* (1300 ppm) > κ^1-*O* (1000 ppm) > η^2-*ON* (400 ppm). Similarly, the value of $C_Q(^{17}O)$ shows the following trend:

(61) Wu, G.; Yamada, K.; Dong, S.; Grondey, H. *J. Am. Chem. Soc.* **2000**, *122*, 4215–4216.
(62) Wu, G.; Dong, S.; Ida, R.; Reen, N. *J. Am. Chem. Soc.* **2002**, *124*, 1768–1777.
(63) Gervais, C.; Dupree, R.; Pike, K. J.; Bonhomme, C.; Profeta, M.; Pickard, C. J.; Mauri, F. *J. Phys. Chem. A* **2005**, *109*, 6960–6969.
(64) Chekmenev, E. Y.; Waddell, K. W.; Hu, J.; Gan, Z.; Wittebort, R. J.; Cross, T. A. *J. Am. Chem. Soc.* **2006**, *128*, 9849–9855.
(65) Waddell, K. W.; Chekmenev, E. Y.; Wittebort, R. J. *J. Phys. Chem. B* **2006**, *110*, 22935–22941.
(66) Kwan, I. C. M.; Mo, X.; Wu, G. *J. Am. Chem. Soc.* **2007**, *129*, 2398–2407.
(67) Pizzotti, M.; Porta, F.; Cenini, S.; Demartin, F.; Masciocchi, N. *J. Organomet. Chem.* **1987**, *330*, 265–278.

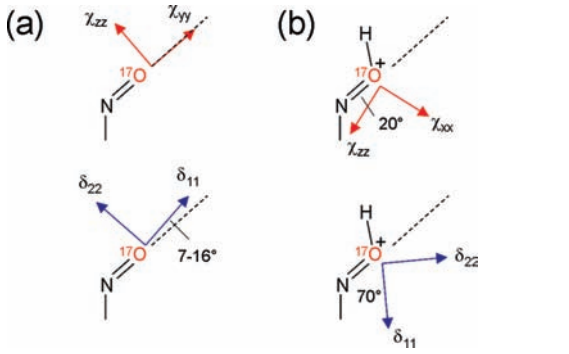

Figure 5. Illustration of the orientations of the ^{17}O QC (top) and CS (bottom) tensors in the molecular frame of reference determined for (a) NODMA, $SnCl_2Me_2(NODMA)_2$, $ZnCl_2(NODMA)_2$ and (b) NODMA·HCl. In (a) and (b), δ_{33} is nearly perpendicular (<18°) and exactly perpendicular to the C−N═O plane, respectively.

η^2-*ON* (14 MHz) > κ^1-*N* (13 MHz) > κ^1-*O* (11 MHz). These results strongly indicate that ^{17}O NMR tensors can be used as a sensitive probe of the binding mode in *C*-nitrosoarene metal complexes.

NMR Tensor Orientations in the Molecular Frame. As mentioned earlier, analyses of ^{17}O NMR spectra can yield only the *relative* orientation between QC and CS tensors. To link the observed NMR tensors to the molecular frame of reference, we often rely on high-level quantum chemical calculations. As discussed in the previous section, a higher degree of accuracy can often be achieved in the calculation of ^{17}O QC tensors. Consequently, it is more reliable to use the computed ^{17}O QC tensor as an internal reference, which then allows us to place experimentally determined ^{17}O CS tensors into the molecular frame of reference. For the *C*-nistrosoarenes under consideration, we found that χ_{zz} is invariantly along the direction of the nonbonding (electron lone pair) orbital. In the cases of NODMA, $SnCl_2Me_2(NODMA)_2$ and $ZnCl_2(NODMA)_2$, this corresponds to the direction lying in the C−N═O plane and perpendicular to the N═O bond. For NODMA·HCl, on the other hand, this direction is within the N═O−H plane making an angle of approximately 20° with respect to the N═O bond. These ^{17}O QC tensor orientations are depicted in Figure 5. It should also be noted that the DFT calculations suggest that $C_Q > 0$ in NODMA, $SnCl_2Me_2(NODMA)_2$, and $ZnCl_2(NODMA)_2$, but $C_Q < 0$ in NODMA·HCl. Once the QC tensor is fixed in the molecular frame, we can use the experimentally determined relative orientation between the QC and CS tensors (Euler angles α, β, γ) to decide on the CS tensor orientation. As shown in Figure 5, the ^{17}O CS tensors in NODMA, $SnCl_2Me_2(NODMA)_2$, and $ZnCl_2(NODMA)_2$ have essentially the same orientation such that δ_{11} is almost along the N═O bond (within 7−16°). The ^{17}O CS tensor for NODMA·HCl has a quite different orientation. In this case, δ_{11} is nearly along the O−H bond direction making an angle of 70° with respect to the N═O bond. A common feature among the ^{17}O CS tensors of the four *C*-nitrosoarenes is that δ_{33} is perpendicular to the C−N═O plane. These tensor orientations are in good agreement with the computed results.

To put the aforementioned NMR tensor orientations in context, we show in Figure 6 what has been known about the ^{17}O QC and CS tensors in several related functional groups. The ^{17}O QC tensor in ozone (O_3) was determined from hyperfine structures observed in rotational spectra.[68,69] Several years ago, Kaupp et al.[70] reported an extensive DFT study of oxyheme

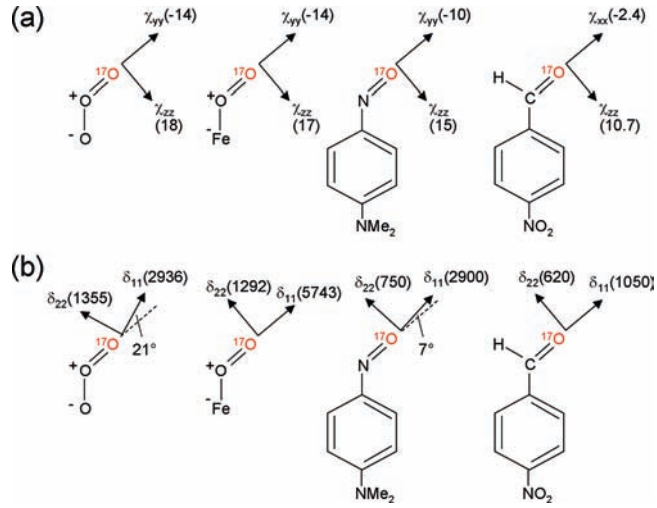

Figure 6. Comparison of ^{17}O (a) QC and (b) CS tensor orientations in several related X = O (X = O, N, C) functional groups. Actual values of the individual tensor components (CS in ppm and QC in MHz) are given in the parentheses. From left to right: ozone, an oxyheme model, NODMA, and *p*-nitrobenzaldehyde. Only one of the resonance structures is shown for ozone and the oxyheme model to emphasize chemical bonding similarity for the terminal oxygen.

model complexes in which they showed that the ^{17}O CS and QC tensor of the O_2 ligand in an oxyheme model have the same orientations as those in O_3. Because an aldehyde group (H−C═O) is isoelectronic with a nitroso group (−N═O), the ^{17}O QC and CS tensors recently observed for *p*-nitrobenzaldehyde[24] were also shown for comparison. Within the series of functional groups shown in Figure 6, χ_{zz} (or C_Q) is invariantly positive with its direction being in-plane and perpendicular to the N═O or C═O bond. In fact, this is also true for most of the carbonyl compounds.[4] Because χ_{zz} is positive, the other two QC tensor components (χ_{yy} and χ_{xx}) must have negative values. Close inspection of the QC tensors in these functional groups reveals that, on going from O_3 to aldehyde, as the magnitude of χ_{zz} decreases, the magnitude of the out-of-plane component *increases* and the component along the X = O bond *decreases*. As a consequence, there is an apparent switch of QC tensor orientation between nitroso and aldehyde groups. This is simply due to the way that these two components are defined (i.e., $|\chi_{yy}| > |\chi_{xx}|$). Aside from this aspect, it is clear that the ^{17}O QC tensors in these functional groups are closely related. Quite interestingly, these functional groups all have very similar ^{17}O CS tensor orientation in the molecular frame, despite the fact that individual CS tensor components are drastically different in magnitude.

It is also interesting to note the ^{17}O QC and CS tensors observed for NODMA are similar to those predicted for the terminal oxygen of O_3 and for the O_2 ligand in oxyheme model complexes.[70] In this context, there exists a long-standing problem in the literature regarding the ^{17}O NMR properties of the O_2 ligand in oxyheme complexes. Oldfield et al.[26] reported the first solid-state ^{17}O NMR study of [$^{17}O_2$] bound to picket fence porphyrin (an oxyheme model), hemoglobin and myoglobin. Their spectral analyses for oxypicket fence porphyrin

(68) Cohen, E. A.; Pickett, H. M. *J. Mol. Struct.* **1983**, *97*, 97–100.
(69) Cohen, E. A.; Hillig II, K. W.; Pickett, H. M. *J. Mol. Struct.* **1995**, *352/353*, 273–282.
(70) Kaupp, M.; Rovira, C.; Parrinello, M. *J. Phys. Chem. B* **2000**, *104*, 5200–5208.

yielded very large ^{17}O chemical shift anisotropy but rather small ^{17}O quadrupole coupling constant ($C_Q < 2$ MHz). As pointed out by Kaupp et al.,[70] the reported solid-state ^{17}O NMR parameters are inconsistent with the solution ^{17}O NMR results reported by Gerothanassis and co-workers.[71,72] To certain extent, our solid-state ^{17}O NMR results for the R−N═O group indirectly support the calculations of Kaupp et al.[70] in that the ^{17}O quadrupole coupling constant for the terminal oxygen of the O_2 ligand in oxyheme complexes should be quite large, on the order of 17 MHz. Of course, this value should be considered as the rigid-lattice value for the O_2 ligand in oxyheme systems. Nonetheless, it appears that simple fast Fe−O_2 axial rotation motion as proposed by Oldfield and co-workers[26,27] can explain some but not all aspects of the experimental observations. Further research is clearly needed in order to solve this puzzle. At least, our new results demonstrate convincingly that it is feasible to obtain high-quality solid-state ^{17}O NMR spectra even when $C_Q(^{17}O)$ is as large as 15 MHz. It would be useful to re-examine solid-state ^{17}O NMR of some oxyheme models at ultrahigh magnetic fields.

Analysis of the ^{17}O Shielding Tensors. In this section, we present a detailed analysis of the ^{17}O shielding tensors in *C*-nitrosoarene compounds using a computational approach. This analysis is performed in two steps. First, we examine shielding contributions from different origins. Second, we analyze the major paramagnetic shielding contributions from individual molecular orbitals (MOs).

According to Ramsey's theory of nuclear shielding,[73] the total shielding tensor at a nucleus can be divided into diamagnetic and paramagnetic contributions:

$$\sigma_{ii} = \sigma_{ii}^{d} + \sigma_{ii}^{p} \tag{4}$$

where the subscript *ii* indicates the individual principal components of the shielding tensor ($i = x, y, z$). For $i = x$, the two shielding contributions can be written as:

$$\sigma_{xx}^{d} = \frac{\mu_0}{4\pi}\frac{e^2}{2m_e^2}\langle 0|\sum_j \frac{(y_j^2 + z_j^2)}{r_j^3}|0\rangle \tag{5}$$

$$\sigma_{xx}^{p} = \frac{\mu_0}{4\pi}\frac{e^2}{2m_e^2}\sum_{k>0}\left[\frac{\langle 0|\sum_j L_{xj} r_j^{-3}|k\rangle\langle k|\sum_j L_{xj}|0\rangle + cc}{E_0 - E_k}\right] \tag{6}$$

where $\langle 0|$ is the ground-state electronic wave function, the sum over k is over all excited electronic states, the sum over j is over all electrons, L_x is the electron orbital angular momentum operator, r_j is the distance between the jth electron and the nucleus of interest, *cc* indicates complex conjugate, E_0 and E_k are the energy values for the ground- and excited-states, respectively, other symbols such as μ_0, e, and m_e are standard constants. Qualitatively, the diamagnetic shielding term is dominated by the core electrons and consequently exhibits little orientation dependence. On the other hand, the paramagnetic shielding contribution is responsible for the anisotropic nature of the shielding tensor. It is clear from eq 6 that the paramagnetic shielding term is inversely proportional to the energy gap between the ground state and the excited state.

In the formulation implemented in the ADF software package, σ^p is further partitioned into three different parts:[74]

$$\sigma^p = \sigma^p(\text{gauge}) + \sigma^p(\text{occ-occ}) + \sigma^p(\text{occ-vir}) \tag{7}$$

where σ^p(gauge), σ^p(occ-occ) and σ^p(occ-vir) describe paramagnetic shielding contributions from the gauge, coupling between occupied and occupied MOs, and coupling between occupied and virtual MOs, respectively. A summary of various contributions to the ^{17}O shielding tensor for *C*-nitrosoarenes is provided in the Supporting Information (Table S8). Several general trends are noted. First, σ^d is essentially isotropic (very little dependence on molecular orientation) and exhibits very little variation among different *C*-nitrosoarene molecules. Second, σ^p(gauge) is generally very small, < 20 ppm. Third, σ^p(occ-occ) has slightly larger values/and variations than does σ^p(gauge), but generally does not exhibit any clear trend. Fourth, σ^p(occ-vir) is the predominant term that accounts for both the orientation dependence within each molecule and the large variations among different molecules. Taking NODMA as an example, σ^p(occ-vir) has a value of −4093 ppm along the N═O bond (σ_{11}) but only −107 ppm along the direction normal to the C−N═O plane (σ_{33}). In comparison, the corresponding σ^p(occ-vir) values in NODMA·HCl are −704 and −169 ppm.

Because σ^p(occ-vir) is the most important source of paramagnetic shielding contribution, we examine it further in order to gain better understanding of the origin of the extreme ^{17}O shielding tensors observed in *C*-nitrosoarenes. It turns out that, for *C*-nitrosoarenes, σ^p(occ-vir) is determined essentially by just a few MO couplings out of a large number of possible MO couplings, making it easier to discuss them in detail. From this point further, we switch our terminology from "MO coupling" to "magnetic field-induced mixing" to emphasis the physical origin of σ^p(occ-vir). Table 3 lists the major contributors to σ^p(occ-vir) along the directions of individual shielding tensor components, together with the relevant energy gap, ΔE.

In the discussion that follows, we use NODMA as an example to illustrate how magnetic field-induced mixing between individual MOs contributes to the ^{17}O shielding tensor. Our discussion is generally within the framework of the Ramsey's theory (eqs 4−6) and at the same time makes use of the results given by Jameson and Gutowsky.[75] To learn more about the general relationship between magnetic field-induced MO mixing and a shielding tensor, the reader may consult an excellent review written by Widdifield and Schurko.[76] Figure 7 shows the four most important MOs with regard to the origin of σ^p(occ-vir). It is interesting to note that the same set of MOs also make the largest contributions to σ^p(occ-vir) at the ^{15}N nucleus within the N═O group. As seen in Figure 7, because a 90° rotation of the n orbital along the N═O bond would generate a significant overlap with the π^*(NO) orbital, this pair of MOs can be "mixed" by the presence of a strong magnetic field along the N═O bond. In addition, because the energy gap between the n and π^*(NO) MOs is very small (1.07 eV in NODMA), magnetic field-induced mixing between these MOs would thus produce a significant amount of σ^p(occ-vir), according to eq 6. In

(71) Gerothanassis, I. P.; Momenteau, M. *J. Am. Chem. Soc.* **1987**, *109*, 6944–6947.
(72) Gerothanassis, I. P.; Momenteau, M.; Loock, B. *J. Am. Chem. Soc.* **1989**, *111*, 7006–7012.
(73) Ramsey, N. F. *Phys. Rev.* **1950**, *78*, 699–703.
(74) Schreckenbach, G.; Ziegler, T. *J. Phys. Chem.* **1995**, *99*, 606–611.
(75) Jameson, C. J.; Gutowsky, H. S. *J. Chem. Phys.* **1964**, *40*, 1714–1724.
(76) Widdifield, C. M.; Schurko, R. W. *Concepts Magn. Reson., Part A* **2009**, *34*, 91–123.

Table 3. Calculated Paramagnetic Shielding Contributions (in ppm) Arising from Magnetic Field-Induced Mixing between Occupied and Virtual MOs, σ^p (occ-vir), along Three Principal ^{17}O Shielding Tensor Components for *C*-Nitrosoarene Compounds[a]

compound	MO mixing	σ_{11}	σ_{22}	σ_{33}	ΔE (eV)[b]
NODMA	σ(NO) → π^*(NO)	16	−249 (30%)	0	8.95
	n → π^*(NO)	−3649 (90%)	−99 (12%)	0	1.07
	n → π^*(NC)	−327 (8%)	0	0	4.14
$SnCl_2Me_2(NODMA)_2$	σ(NO) → π^*(NO)	−1	−163 (20%)	−1	9.13
	n → π^*(NO)	−1868 (83%)	−17 (2%)	1	1.63
	n → π^*(NC)	−105 (5%)	0	−1	4.69
$ZnCl_2(NODMA)_2$	σ(NO) → π^*(NO)	6	−176 (22%)	0	8.90
	n → π^*(NO)	−1795 (78%)	8 (1%)	−43	1.50
	n → π^*(NC)	−78 (3%)	−1	0	4.32
NODMA·HCl	σ(NO) → π^*(NO)	−16	−72 (26%)	0	10.5
	n → π^*(NO)	−275 (40%)	−77 (28%)	0	2.94
	n → π^*(NC)	−60 (4%)	−18 (6%)	0	6.11

[a] Percentage contributions shown in parentheses are defined as σ^p(occ-vir)/σ^p(total) for each shielding tensor component. [b] Averaged values if several nearly degenerate MOs exist.

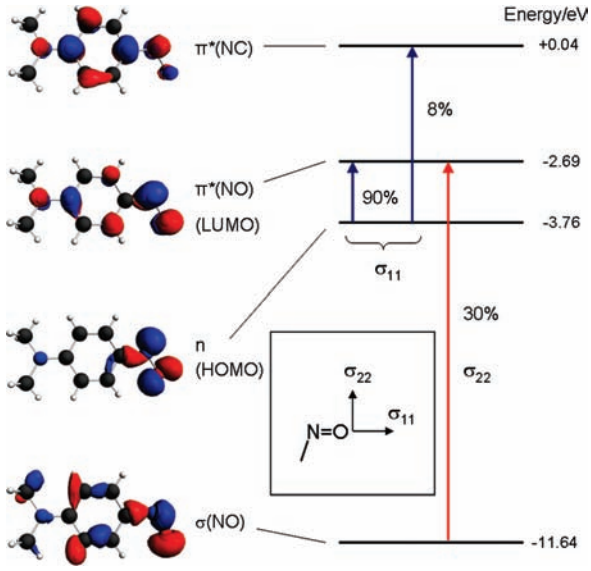

Figure 7. Selected occupied and virtual MOs that have the largest paramagnetic shielding contributions and their associated energy levels for NODMA.

comparison, the MO mixing between n and π^*(NC) has the same symmetry, but a much larger ΔE (3.80 eV) and, thus, much smaller σ^p(occ-vir). Another factor is that π^*(NC) is not localized as much as π^*(NO) around the oxygen atom. However, as seen in Figure 7 and Table 3, the n → π^* type of MO mixing accounts for 98% of the total paramagnetic shielding along the direction of σ_{11}. In contrast, the σ → π^* mixing is responsible for σ^p(occ-vir) along the direction that is in-plane but perpendicular to the N═O bond (the direction of σ_{22}). As seen from Table 3, the contribution from n → π^* mixing decreases to 88% in $SnCl_2Me_2(NODMA)_2$, to 78% in $ZnCl_2(NODMA)_2$, and 44% in NODMA·HCl. This decrease is primarily due to the increase in energy gap between the two MOs. As expected from eq 6, σ^p depends linearly on $1/\Delta E$ for both n → π^* and σ → π^* mixing, as illustrated in Figure S2 in the Supporting Inforamtion. The similar slopes observed for the two types of mixing suggest that the degrees of MO overlaps are similar for n → π^* and σ → π^*. An approximately linear relationship between ^{17}O chemical shifts and lowest-energy electronic transitions measured in optical spectra was first observed in the early years of ^{17}O NMR spectroscopy.[77] However, caution should be exercised if one uses this line of reasoning to interpret chemical shifts, i.e., to link the observed isotropic chemical shift to a particular electronic transition. In principle, as we showed here, it is the individual shielding tensor components rather than the trace of the shielding tensor that should be correlated to the electronic transitions.

For the Zn and Sn complexes of NODMA, the O → M bonding is essentially σ-donation from the ligand molecule. A natural bond orbital (NBO) analysis suggests that there is very little back-donation from the metal orbitals to the π^* MO of the N═O group. Therefore, it is not surprising that the two metal complexes exhibit rather similar ^{17}O NMR parameters.

Townes−Dailey Analysis of the ^{17}O QC Tensors. In this section, we describe results from a Townes−Dailey analysis[78] of the observed ^{17}O QC tensors for *C*-nitrosoarenes. For NODMA, $SnCl_2Me_2(NODMA)_2$, and $ZnCl_2(NODMA)_2$, we used the expressions derived by Brown and co-workers[79–81] for treating N−O-containing compounds:

$$\chi_{zz} = (2 - {}^1/_2P_\pi - {}^1/_2P_\sigma)\chi_0 \quad (8)$$

$$\chi_{yy} = (-1 - {}^1/_2P_\pi + P_\sigma)\chi_0 \quad (9)$$

$$\chi_{xx} = (-1 + P_\pi - {}^1/_2P_\sigma)\chi_0 \quad (10)$$

where χ_{zz} and χ_{yy} are the ^{17}O QC tensor components that are perpendicular and parallel to the N═O bond, respectively; χ_{xx} is the ^{17}O QC tensor component normal to the C−N═O plane; $\chi_0 = +20.9$ MHz, corresponding to the ^{17}O quadrupole coupling constant from a single electron in a pure 2p atomic orbital; P_π and P_σ are the orbital populations in the π and σ bonds of the N═O group, respectively.

For NODMA·HCl, because the oxygen atom of interest is dicoordinated (N═O−H), a slightly different model has to be used. If we assume that the oxygen atom in question has sp^2 hybrid orbitals within the plane forming two σ bonds and a lone pair and a pure 2p orbital normal to the N═O−H plane contributing to a π bond, we can obtain the following expressions for the ^{17}O QC tensor components:[58,82,83]

$$\chi_{zz} = [-{}^1/_2P_\pi + {}^1/_2(2 - s)P_\sigma + {}^1/_2(s - 1)P_{LP}]\chi_0 \quad (11)$$

$$\chi_{yy} = [P_\pi - {}^1/_2(s + 1)P_\sigma + {}^1/_2(s - 1)P_{LP}]\chi_0 \quad (12)$$

$$\chi_{xx} = [-{}^1/_2P_\pi + {}^1/_2(2s - 1)P_\sigma + (1 - s)P_{LP}]\chi_0 \quad (13)$$

where χ_{zz} and χ_{xx} are the ^{17}O QC tensor components that are in the N═O−H plane with χ_{xx} nearly bisecting the N═O−H angle; χ_{yy} is the ^{17}O QC tensor component normal to the N═O−H

Table 4. Experimental N−O Bond Lengths, NBO Atomic Charges, Oxygen Orbital Populations from a Townes−Dailey Analysis of the Experimental ^{17}O QC Tensors, and Calculated Mayer Bond Orders for *C*-Nitrosoarene Compounds

			Townes−Dailey analysis			ADF calculation
compound	r_{NO}/Å	Q_O(e)	P_π	P_σ	π bond order[a]	Mayer bond order
NODMA	1.247	−0.3938	1.362	1.202	0.709	1.64
$SnCl_2Me_2(NODMA)_2$	1.296	−0.4980	1.639	1.356	0.400	1.47
$ZnCl_2(NODMA)_2$	1.304	−0.5719	1.694	1.388	0.340	1.40
NODMA·HCl	1.374	−0.4783	1.835	1.248	0.183	1.04

[a] The π bond order $= (2 - P_\pi)/0.9$ as suggested by Brown and co-workers.[79–81]

plane; P_π is the orbital populations in the N═O π bond; P_σ is the averaged orbital population in the N−O and O−H σ bonds; P_{LP} is the orbital population for the electron lone pair within the N═O−H plane ($P_{LP} = 2$); s is the s-character in the sp^2 hybrid orbitals. In this study, we used $s = 0.406$ for NODMA·HCl, assuming that the N═O−H angle is 115°.

Applying eqs 8−13 to the experimental ^{17}O QC tensor components, we obtained orbital populations for *C*-nitrosoarenes; see Table 4. In general, on going from NODMA, $SnCl_2Me_2(NODMA)_2$, $ZnCl_2(NoDMA)_2$ to NODMA·HCl, we observe an increase in P_π, thus a decrease in the π bond order. This is in agreement with the observed trend in the N═O bond length. Furthermore, the π bond order can be calculated from P_π using $(2 - P_\pi)/0.9$ where the factor of 0.9 arises from a consideration of the electronegativity difference between N and O atoms, as described by Brown and co-workers.[79–81] Table 4 also lists the calculated Mayer bond order for the four *C*-nitrosoarenes. Quite interestingly, the Mayer bond orders are in good correlation with the π bond orders. In fact, if we assume that the σ bond order is approximately 1 in the N═O bond, the total bond order (a simple sum of the π and σ bond orders) is in excellent agreement with the calculated Mayer bond order.

For completeness, we also performed a Townes−Dailey analysis of the ^{14}N QC tensor experimentally determined for NODMA.[50] Assuming $\chi_0 = -11$ MHz for a single electron in a pure 2p atomic orbital of the neutral nitrogen atom,[84,85] we obtained $P_\pi = 1.099$ and $P_\sigma = 1.272$ for the N═O bond in NODMA. If we use exactly the same electronegativity argument as mentioned earlier, a π bond order of 0.819 can be calculated using $(2 - P_\pi)/1.1$. This value is in satisfactory agreement with that derived from the ^{17}O QC tensor as shown in Table 4. An NBO analysis indicates that the oxygen atomic charge increases on going from NODMA to its Sn and Zn complexes, consistent with the picture that the κ^1-*O*-binding mode is associated with increased contributions from a dipolar quinonoid resonance structure. The NBO analysis also confirms that the oxygen atom in NODMA·HCl is involved in a quite different orbital hybridization compared with those in the other three *C*-nitrosoarene compounds investigated in this study.

Relationship between ^{17}O QC and CS Tensors. More than three decades ago, Mason[86] demonstrated a correlation between ^{14}N chemical shifts and nuclear quadrupole coupling constants in nitroso compounds. This is because both quantities depend on the imbalance of orbital populations around the atom of interest, as first pointed out by Saika and Slichter[87] and later elaborated by Karplus and Das.[88] There are also several other studies in the literature reporting on similar correlations.[89–91] However, almost all the previous studies have focused only on isotropic chemical shifts. A careful examination of the complete CS and QC tensors under question will definitely provide new insights into the origin of such correlations. Because the imbalance of orbital populations is intrinsically related to the bond order, it is expected that both ^{17}O chemical shift and nuclear quadrupole coupling constant are also correlated to the bond order.[1,92] Indeed, in a previous solid-state ^{15}N NMR study of *C*-nitrosoarenes, Oldfield and co-workers[13] observed a linear relationship between δ_{11} of the ^{15}N CS tensor and the Mayer bond order of the N═O group. In this study, we employ a slightly different approach to examine a similar correlation between ^{17}O CS tensor components and the N═O bond order. In particular, we have obtained the values of π bond order for the *C*-nitrosoarenes from a Townes−Dailey analysis of the ^{17}O QC tensors, as discussed in the previous section. These π bond orders can be considered as "experimental values". As seen from Figure 8, when the ^{17}O CS tensor components are plotted against the π bond order for *C*-nitrosoarenes, a clear trend is observed. That is, δ_{11} and δ_{22} are strongly correlated with the π bond order, but δ_{33} is essentially invariant. As a result, $\delta_{iso}(^{17}O)$ also increases with the π bond order, as first noted by Kidd more than 40 years ago.[93] Recently, we reported a quite general correlation between ^{17}O CS tensor components and C_Q for carbonyl compounds.[4,24] While direct comparison of C_Q is valid within a class of closely related molecules, the underlying assumption is that these molecules have the same ^{17}O QC tensor orientation in the molecular frame of the C═O moiety. When the ^{17}O QC tensor orientation is different or the sign of C_Q is changed, which is the case for the four *C*-nitrosoarenes studied here, it will not be very useful if one examines only the magnitude of C_Q. Therefore, it is much more important and fundamentally correct to examine the nature of chemical bonding by analyzing the full ^{17}O QC tensor (e.g., using the Townes−Dailey model). The trend observed in Figure 8 suggests that the ^{17}O CS and QC tensors in *C*-nitrosoarenes are intrinsically related through the π bond order of the N═O bond. Moreover, the

(77) Figgis, B. N.; Kidd, R. G.; Nyholm, R. S. *Proc. R. Soc. London, A* **1962**, *269*, 469–480.
(78) Townes, C. H.; Dailey, B. P. *J. Chem. Phys.* **1949**, *17*, 782–796.
(79) Cheng, C. P.; Brown, T. L. *J. Am. Chem. Soc.* **1980**, *102*, 6418–6421.
(80) Hiyama, Y.; Brown, T. L. *J. Phys. Chem.* **1981**, *85*, 1698–1700.
(81) Woyciesjes, P. M.; Janes, N.; Ganapathy, S.; Hiyama, Y.; Brown, T. L.; Oldfield, E. *Magn. Reson. Chem.* **1985**, *23*, 315–321.
(82) Brosnan, S. G. P.; Edmonds, D. T.; Poplett, I. J. F. *J. Magn. Reson.* **1981**, *45*, 451–60.
(83) Janes, N.; Oldfield, E. *J. Am. Chem. Soc.* **1986**, *108*, 5743–5753.
(84) Schirmacher, A.; Winter, H. *Phys. Rev. A* **1993**, *47*, 4891–4907.
(85) Tokman, M.; Sundholm, D.; Pyykko, P.; Olsen, J. *Chem. Phys. Lett.* **1997**, *265*, 60–64.
(86) Mason, J. *J. Chem. Soc., Faraday Trans. 2* **1976**, *72*, 2064–2068.
(87) Saika, A.; Slichter, C. P. *J. Chem. Phys.* **1954**, *22*, 26–28.
(88) Karplus, M.; Das, T. P. *J. Chem. Phys.* **1961**, *34*, 1683–1692.
(89) Bancroft, G. M.; Clark, H. C.; Kidd, R. G.; Rake, A. T.; Spinney, H. G. *Inorg. Chem.* **1973**, *12*, 728–731.
(90) Jones, C. H. W.; Sharma, R. D. *J. Chem. Phys.* **1987**, *86*, 5294–5299.
(91) Chung, S. C.; Chan, J. C. C.; Auyeung, S. C. F.; Xu, X. *J. Phys. Chem.* **1993**, *97*, 12685–12690.
(92) Gerothanassis, I. P. Oxygen-17 NMR. In *Encyclopedia of Nuclear Magnetic Resonance*; Grant, D. M., Harris, R. K., Eds. Wiley: New York, 1996; Vol. 5, pp 3430−3440.
(93) Kidd, R. G. *Can. J. Chem.* **1967**, *45*, 605–608.

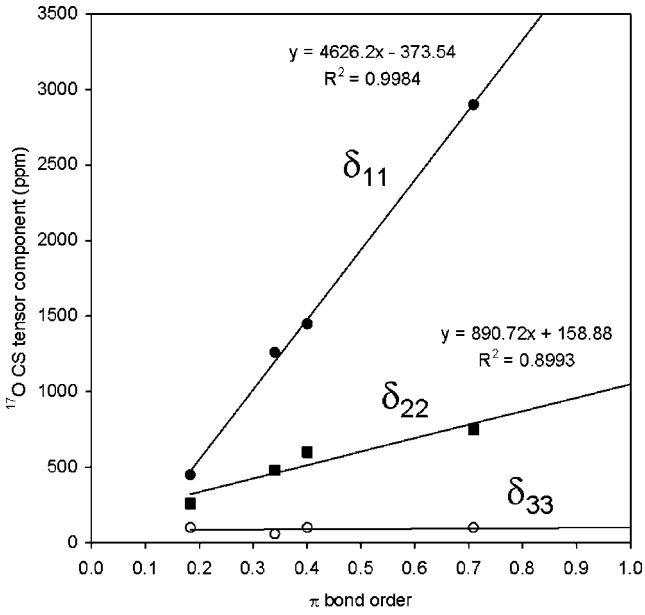

Figure 8. Relationship between ^{17}O CS tensor components and π bond order for *C*-nitrosoarenes.

different slopes observed for δ_{11} and δ_{22} reflect the influence from ΔE. Clearly, the approach illustrated in Figure 8 can be generalized and applied to other functional groups.

Parallelism between ^{17}O and ^{15}N CS Tensors. Previous solution NMR studies have strongly suggested that there exists a parallelism between ^{17}O and ^{15}N chemical shifts for nitroso compounds (X−N═O).[15,94] Now combining our solid-state ^{17}O NMR data with the ^{15}N CS tensors reported by Oldfield and co-workers[13] for *C*-nitrosoarenes, we have an opportunity for the first time to be able to examine the parallelism between ^{17}O and ^{15}N CS tensor components rather than just the isotropic chemical shifts. Figure 9a illustrates the correlation between ^{17}O and ^{15}N CS tensor components for *C*-nitrosoarenes. Clearly, the previously found correlation between isotropic ^{17}O and $^{14/15}$N chemical shifts results exclusively from correlations between only two of the CS tensor components, δ_{11} and δ_{22}. For completeness, Figure 9b also shows the correlation observed for isotropic chemical shifts including both solid-state and solution NMR data. These data can be fitted by a straight line of slope 1.8. It is often argued in the literature that this slope of 1.8 is in excellent agreement with the expected ratio of $\langle 1/r^3\rangle_{2p}$ between O and N atoms, i.e., $\langle 1/r^3\rangle_{2p}(O)/\langle 1/r^3\rangle_{2p}(N) = 1.75$.[95] This type of rationalization stems from the use of the Karplus−Pople equation to describe the paramagnetic shielding contribution:[96]

$$\sigma^{p} = -\frac{\mu_0}{4\pi}\frac{e^2}{2m_e^2}\frac{1}{\Delta E}\langle 1/r^3\rangle_{2p}\sum Q_{AB} \qquad (14)$$

where ΔE is the average electronic excitation energy and $\sum Q_{AB}$ is a summation of the charge density-bond order matrix elements. According to eq 14, σ^p depends on $\langle 1/r^3\rangle_{2p}$ for nitrogen and oxygen. However, although it is clear that $\langle 1/r^3\rangle_{2p}$ (as well as $\langle 1/r^3\rangle_d$) is indeed a valid measure of the chemical shift *range*

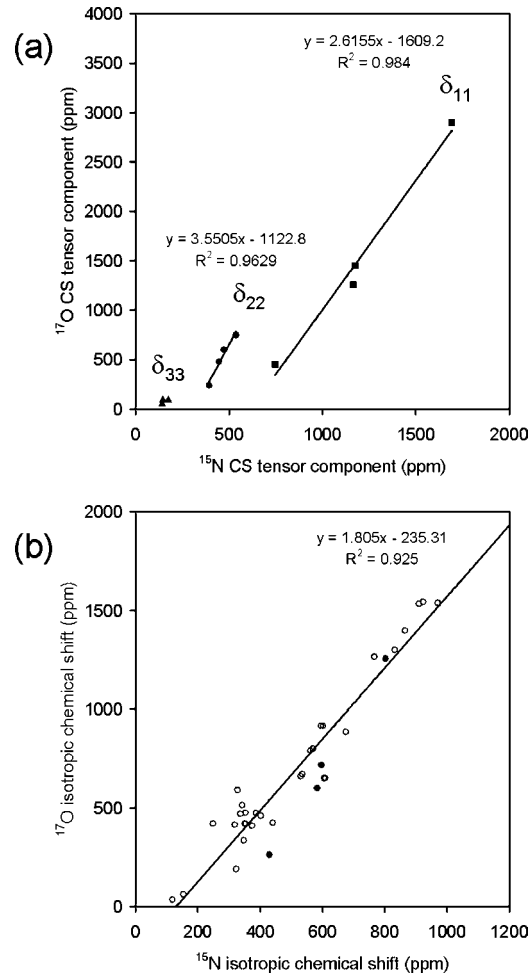

Figure 9. (a) Correlation between ^{17}O and ^{15}N CS tensor components observed for the four *C*-nitrosoarene compounds investigated in this study. (b) Correlation between isotropic ^{17}O and ^{15}N chemical shifts determined from both solid-state NMR (solid circles) and solution-state NMR (open circles) experiments for nitroso compounds (X−N═O where X = R, Ar, SR, Halide, OR, NR_2). Solution NMR data were obtained from refs 15 and 94. All $^{14/15}$N chemical shifts were referenced to that of liquid NH_3, $\delta = 0$ ppm.

when chemical shifts for different elements are compared as demonstrated by Jameson and Gutowsky,[75] several other factors will need to be considered for comparing CS tensor components between two nuclei within the same functional group (e.g., ^{15}N and ^{17}O in the N═O group). As seen from Figure 9, when the δ_{11} and δ_{22} components are examined, the observed slopes, 2.62 and 3.55, are larger than 1.75. This suggests that the other two factors (ΔE and $\sum Q_{AB}$) in eq 14 must be important. For the *C*-nitrosoarenes under investigation, our calculations show that the same set of MOs are responsible for both ^{15}N and ^{17}O paramagnetic shielding contributions. Thus the ΔE term will be identical when applying eq 14 to either ^{15}N or ^{17}O nuclei. Under such a circumstance, the observed discrepancy in slopes (2.62 versus 1.75 for δ_{11} and 3.55 versus 1.75 for δ_{22}) must reflect the subtle difference in $\sum Q_{AB}$. The fact that both the observed slopes are greater than 1.75 suggests that changes in $\sum Q_{AB}$ are larger for oxygen than for nitrogen. Because the paramagnetic shielding contribution along the direction of δ_{33} is negligible, neither $\delta_{33}(^{17}O)$ nor $\delta_{33}(^{15}N)$ shows much variation among different compounds.

(94) Andersson, L.-O.; Mason, J. *J. Chem. Soc., Dalton Trans.* **1974**, 202–205.
(95) Barnes, R. G.; Smith, W. V. *Phys. Rev.* **1954**, *93*, 95–98.
(96) Karplus, M.; Pople, J. A. *J. Chem. Phys.* **1963**, *38*, 2803–2807.

4. Conclusion

In this study, we have used solid-state ^{17}O NMR spectroscopy to determine the ^{17}O QC and CS tensors in four representative *C*-nitrosoarene compounds. This is the first time that such fundamental ^{17}O NMR tensors have been measured for this important class of organic compounds. The observed ^{17}O QC and CS tensors exhibit remarkable sensitivity toward the chemical bonding scheme at the nitroso group (−N═O). The ^{17}O quadrupole coupling constant and chemical shift anisotropy observed in *C*-nitrosoarenes are among the largest values yet measured for oxygen-containing organic functional groups by solid-state ^{17}O NMR. Our success in acquiring high-quality solid-state ^{17}O NMR spectra for this challenging class of compounds provides strong evidence that all oxygen-containing functional groups should be accessible by solid-state ^{17}O NMR spectroscopy at ultrahigh magnetic fields (e.g., 21 T). In addition to reporting new experimental ^{17}O NMR results, we have also performed extensive DFT calculations. The computed ^{17}O NMR tensors are in reasonable agreement with the observed values. We have presented a detailed analysis of various MO contributions to the shielding tensor at the oxygen nucleus. We have analyzed the ^{17}O QC tensors using the Townes−Dailey model and found that the ^{17}O CS and QC tensors in *C*-nitrosoarenes are intrinsically related through the π bond order of the N═O group. We have also examined the strong parallelism between ^{17}O and ^{15}N CS tensor components (δ_{11} and δ_{22}). This parallelism arises from the fact that the shielding at both oxygen and nitrogen nuclei of the nitroso (N═O) moiety is dominated by the magnetic field-induced mixing of the n $\rightarrow \pi^*$ and $\sigma \rightarrow \pi^*$ nature. Our computational results also suggest that ^{17}O NMR tensors are remarkably sensitive to the binding mode of *C*-nitrosoarene/metal complexes. The new results obtained in this study on *C*-nitrosorenes and their metal complexes have laid a solid foundation for future solid-state ^{17}O NMR studies of *C*-nitrosoarenes bound to globin proteins. Further research in this direction is underway in our group.

Acknowledgment. This work was supported by the Natural Sciences and Engineering Research Council (NSERC) of Canada. Quantum chemical calculations were performed at the High Performance Computing Virtual Laboratory (HPCVL) at Queen's University. We thank Dr. Hartmut Schmider for assistance in performing ADF calculations. Access to the 900 MHz NMR spectrometer was provided by the National Ultrahigh Field NMR Facility for Solids (Ottawa, Canada), a national research facility funded by the Canada Foundation for Innovation, the Ontario Innovation Trust, Recherche Québec, the National Research Council Canada, and Bruker BioSpin and managed by the University of Ottawa (www.nmr900.ca). NSERC is acknowledged for a Major Resources Support grant.

Supporting Information Available: Complete citation of reference 36; detailed crystallographic and structural data for $SnCl_2Me_2(NODMA)_2$ (atomic coordinates, bond lengths, bond angles, torsion angles, and hydrogen coordinates) and crystallographic information file in CIF format; complete list of computational results. This material is available free of charge via the Internet at http://pubs.acs.org.

JA909656W